We are IntechOpen, the world's leading publisher of Open Access books
Built by scientists, for scientists

6,900
Open access books available

185,000
International authors and editors

200M
Downloads

Our authors are among the

154
Countries delivered to

TOP 1%
most cited scientists

12.2%
Contributors from top 500 universities

CLARIVATE ANALYTICS
BOOK CITATION INDEX
INDEXED

WEB OF SCIENCE™

Selection of our books indexed in the Book Citation Index
in Web of Science™ Core Collection (BKCI)

Interested in publishing with us?
Contact book.department@intechopen.com

Numbers displayed above are based on latest data collected.
For more information visit www.intechopen.com

Distribution Diagrams and Graphical Methods to Determine or to Use the Stoichiometric Coefficients of Acid-Base and Complexation Reactions

Alberto Rojas-Hernández[1], Norma Rodríguez-Laguna[1],
María Teresa Ramírez-Silva[1] and Rosario Moya-Hernández[2]
[1]Depto. de Química, Área de Química Analítica,
Universidad Autónoma Metropolitana-Iztapalapa,
[2]Facultad de Estudios Superiores-Cuautitlán, Lab. 10, UIM,
*Universidad Nacional Autónoma de México,*
Mexico

1. Introduction

Graphical methods to study the behaviour of systems showing different chemical equilibrium are known and very used in several fields of Chemistry (particularly in Bioinorganic, Medicinal and Pharmaceutical Chemistry) in order to establish the chemical species that are related with drugs behaviour in different systems. Among these methods, the most commonly used are the distribution diagrams (Högfeldt, 1979), the titration curves (Asuero & Michałowski, 2011) and the molar ratio and continuous variations methods (Hartley et al., 1980).

In the present work we have selected two molecules used extensively like drugs. In order to exemplify some novelties related with distribution diagrams and titration curves for acid-base systems we have selected the case of oxine (HOX, 8-hydroxiquinoline) that has been used as antiseptic and disinfectant. On the other hand, we have selected the complexation interaction between Fe(III) and tenoxicam (Tenox) to show other novelties related with more complicated distribution diagrams and molar ratio and continuous variations methods, because tenoxicam has been extensively used as non-steroidal anti-inflammatory drug that may be complexed with several metal ions. The chemical developed formulae of these compounds are presented in Scheme 1.

2. Distribution diagrams for acid-base and complexation systems

Graphic representations of chemical systems have found wide application because a simple look at them allows for solve specific problems and have a panorama, qualitative and quantitative, for different problems and phenomena. Moreover, some of these representations also permit to graphically solve the stated problem with a predetermined error (Vicente-Pérez, 1985). Distribution diagrams of species are some of the most used

graphic representations since the second half of 20th century; nevertheless, there have been some novelties on the field in the last decade (e.g. Moya-Hernández et al., 2002a, 2002b).
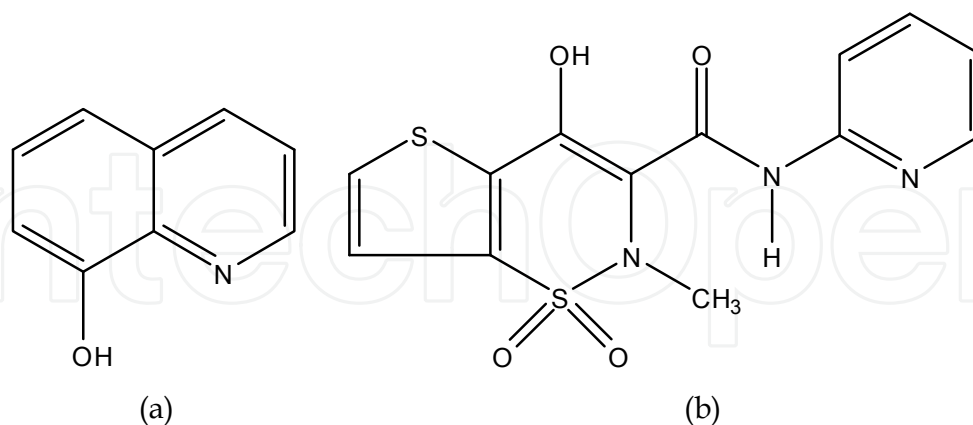

Scheme 1. Developed formulae of a) oxine (HOX) and b) tenoxicam (Tenox).

2.1 Typical representations of distribution diagrams

In this section some typical representations will be quickly reviewed to introduce the newest representations given in section 2.2.

2.1.1 Acid-base systems

In Chemistry the study of polyprotic systems, whose global formation equilibrium are represented in Eq. 1, is of crucial importance, because many substances, drugs among them, follow this Brфnsted acid-base behaviour.

$$L^{a-} + jH^+ \rightleftharpoons LH_j^{j-a} \quad \text{with} \quad \beta_j = \frac{[LH_j^{j-a}]}{[L^{a-}][H^+]^j} \tag{1}$$
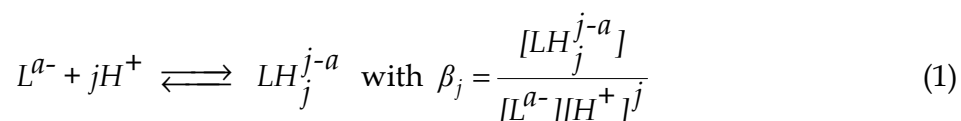
The typical way to define the molar fractions to describe the species distribution of the component L in this system with respect to the proton (H^+) is given in Eq. 2, as well as its factorization in the substance amount balance equation of this component in the system – using the set of Eq. 1 (Rojas-Hernández, 1995).

$$f_j = \frac{[LH_j^{j-a}]}{[L]_T} = \frac{\beta_j[H^+]^j}{1 + \sum_{j=1}^{n} \beta_j[H^+]^j} \tag{2}$$

where $[L]_T$ is L total concentration in the system.

An example of distribution diagram is given in Fig. 1a, showing the case of oxine hydrochloride (H_2OXCl, 8-hydroxiquinolinol = HOX).

Fig. 1b represents the function known as Average Proton Number ($\bar{n}$), introduced and developed by Niels and Jannik Bjerrum (Hartley et al., 1980). Eq. 3 shows the definition and

factorization of $\bar{n}$ as a function of pH (taking into account the sets of Eq. 1 and 2) for aqueous solutions.

$$\bar{n} = \frac{[H^+]_T - [H^+]}{[L]_T} = \frac{\sum_{j=1}^{n} j\beta_j[H^+]^j}{1 + \sum_{j=1}^{n} \beta_j[H^+]^j} = \sum_{j=1}^{n} jf_j \tag{3}$$

$[H^+]_T$ is the protons total concentration in the system, which requires the balance of proton equation. In aqueous solutions, this equation needs the autoprotolysis constant and special considerations.

The chemical information given in the curves of Fig. 1 is the same, as expected from Eq. 2 and 3. In fact, the Average Proton Number is the set of statistical means of the subjacent distributions resumed by the distribution diagram of Fig. 1, as it will be explained in the section 2.2.
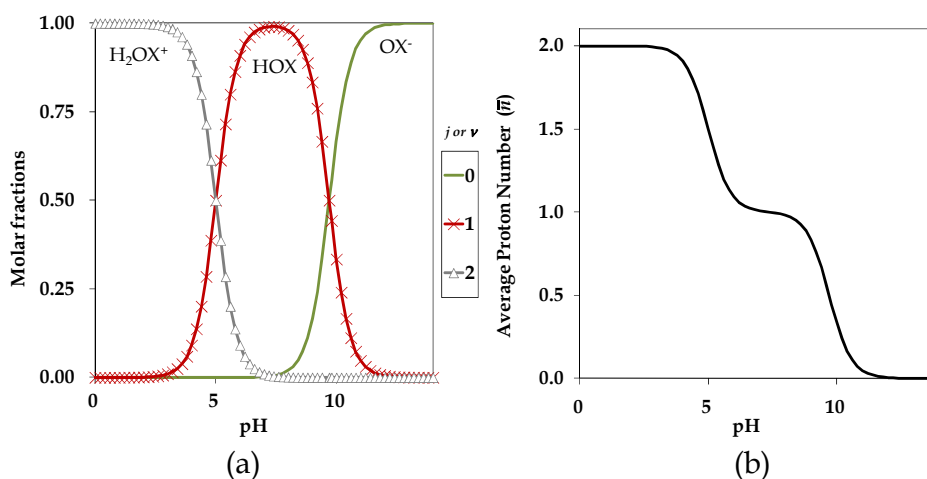

Fig. 1. Typical graphic representations of the oxine hydrochloride (H$_2$OXCl) in water as a function of pH. j (or ν) represents the proton stoichiometric coefficient for each species.
a) Distribution diagram. b) Average proton number. Data were taken from Ringbom (1963): pK_{a1} = 5.0, pK_{a2} = 9.7.

2.1.2 Complexation systems

Even though the knowledge of Brønsted acid-base behaviour is important, the interaction of substances with metal ions is remarkable as well (e.g., the interaction of drugs with metal ions may potentiate or suppress its pharmacological activity or toxicity).

The formation of several coordination compounds, or complexes, between a metal ion (M) and a ligand (L) can be described by the global formation equilibrium represented in Eq. 4.

$$iM + jL \xrightleftharpoons{\qquad} M_iL_j \text{ with } \beta_{ij} = \frac{[M_iL_j]}{[M]^i[L]^j} \tag{4}$$
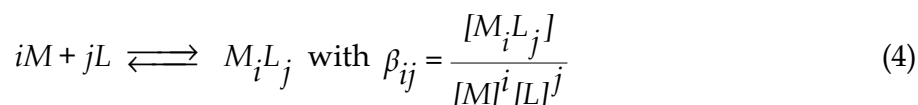
where $i \in \{1, 2, ..., m\}$ and $j \in \{(0, 1, ..., n[i]\}$

In Eq. 4, the charge of the species has been omitted for notation simplicity. When $i = 1$ the complexes are called mononuclear, but when $i \geq 2$ the corresponding complexes are called polynuclear. The formation of polynuclear complexes on a given system is thermodynamically favoured when the total concentration of M ($[M]_T$) is high and placed over the mononuclear wall (Ringbom, 1963).

In complexation chemistry, several distributions have to be considered. In general, it is preferred to study the way the component L is distributing on M species, but studying how the component M is distributing on L species may be interesting as well. In both cases there are two possible descriptions, depending on what is considered between the amount or the concentrations of the species. When polynuclear compexes are formed in the system all the distribution diagrams representing the formation of the species depends on $[M]_T$ and $[L]_T$.

Distributions of L in M

The M substance amount fractions are defined by Eq. 5.

$$^{L/M}f_{10} = \frac{[M]}{[M]_T} = \frac{1}{1 + \sum_{i=1}^{m}\left(\sum_{j=0}^{n[i]} i\beta_{ij}[M]^{(i-1)}[L]^{j}\right)}$$

$$\text{and} \quad {}^{L/M}f_{ij} = \frac{i[M_iL_j]}{[M]_T} = {}^{L/M}f_{10}\left(i\beta_{ij}[M]^{(i-1)}[L]^{j}\right) \tag{5}$$

where $i \in \{1, 2, ..., m\}$ and $j \in \{0, 1, ..., n[i]\}$

When polynuclear M species are not forming in a given system ($i = 1$), this distribution only depends on $[L]_T$, but when polynuclear species appear, the substance amount fractions depend on $[L]_T$ and $[M]_T$; furthermore in this last case the simple sum of the concentrations of M species (Σ_M) is lower than $[M]_T$, in agreement with Eq. 6.

$$\Sigma_M = \sum_{i=1}^{m}\left(\sum_{j=0}^{n[i]}[M_iL_j]\right) < \sum_{i=1}^{m}\left(\sum_{j=0}^{n[i]} i[M_iL_j]\right) = [M]_T \tag{6}$$

In this particular case, M concentration fractions can be defined by Eq. 7.

$$^{L/M}\varphi_{10} = \frac{[M]}{\Sigma_M} = \frac{1}{1 + \sum_{i=1}^{m}\left(\sum_{j=0}^{n[i]}\beta_{ij}[M]^{(i-1)}[L]^{j}\right)} \quad \text{and} \quad {}^{L/M}\varphi_{ij} = \frac{[M_iL_j]}{\Sigma_M} = {}^{L/M}\varphi_{10}\left(\beta_{ij}[M]^{(i-1)}[L]^{j}\right) \tag{7}$$

where $i \in \{1, 2, ..., m\}$ and $j \in \{0, 1, ..., n[i]\}$

The substance amount and concentration fractions of M species are related by means of Eq. 8.

$$^{L/M}\varphi_{ij} = {}^{L/M}f_{ij}\frac{[M]_T}{\Sigma_M} \tag{8}$$

Distributions of M in L

Following the same approach, several distributions of L species may be defined. Then, the L substance amount fractions are defined in Eq. 9, while the L concentration fractions are described in Eq. 10.

$$^{M/L}f_{01} = \frac{[L]}{[L]_T} = \frac{1}{1 + \sum_{j=1}^{n}\left(\sum_{i=0}^{m[j]} j\beta_{ij}[M]^i[L]^{(j-1)}\right)} \tag{9}$$

$$\text{and} \quad ^{M/L}f_{ij} = \frac{j[M_iL_j]}{[L]_T} = {}^{M/L}f_{01}(j\beta_{ij}[M]^i[L]^{(j-1)})$$

where $i \in \{0, 1, ..., m[j]\}$ and $j \in \{1, 2, ..., n\}$

$$^{M/L}\varphi_{01} = \frac{[L]}{[L]_T} = \frac{1}{1 + \sum_{j=1}^{n}\left(\sum_{i=0}^{m[j]} j\beta_{ij}[M]^i[L]^{(j-1)}\right)} \tag{10}$$

$$\text{and} \quad ^{M/L}\varphi_{ij} = \frac{j[M_iL_j]}{[L]_T} = {}^{M/L}\varphi_{01}(j\beta_{ij}[M]^i[L]^{(j-1)})$$

where $i \in \{0, 1, ..., m[j]\}$ and $j \in \{1, 2, ..., n\}$

The substance amount and concentration fractions of L species are related by means of Eq. 11.

$$^{M/L}\varphi_{ij} = {}^{M/L}f_{ij}\frac{[L]_T}{\Sigma_L} \tag{11}$$

because the following inequality is always confirmed.

$$\Sigma_L = \sum_{j=1}^{n}\left(\sum_{i=0}^{m[j]}[M_iL_j]\right) < \sum_{j=1}^{n}\left(\sum_{i=0}^{m[j]} j[M_iL_j]\right) = [L]_T \tag{12}$$

Distribution diagrams for the Fe(III)-tenoxicam system in acetone

In order to exemplify the typical distributions diagrams of M and L species, Fig. 2 is reported for the Fe(III) - tenoxicam (Tenox) system in acetone from previously reported data by Moya-Hernández et al. (2009). The equilibrium constants of this reference have been collected in Table 1.

Species	i	j	$\log\beta_{ij}$
Fe_2Tenox	2	1	9.04 ± 0.03
Fe_2Tenox_2	2	2	14.75 ± 0.06
Fe_2Tenox_3	2	3	18.45 ± 0.07

Table 1. Global formation constants of Fe(III)-tenoxicam species in acetone (Moya-Hernández et al., 2009).

The distribution diagrams that represent the substance amount fractions, calculated from global formation constants given in Table 1, have been constructed with the aid of program MEDUSA (Puigdomenech, 2010). The distribution diagrams that represent the concentration fractions have been obtained by means of Excel (*Microsoft®*) worksheets applying Eq. 8 and 11. Some of the typical distribution diagrams are shown in Fig. 2 and 3.
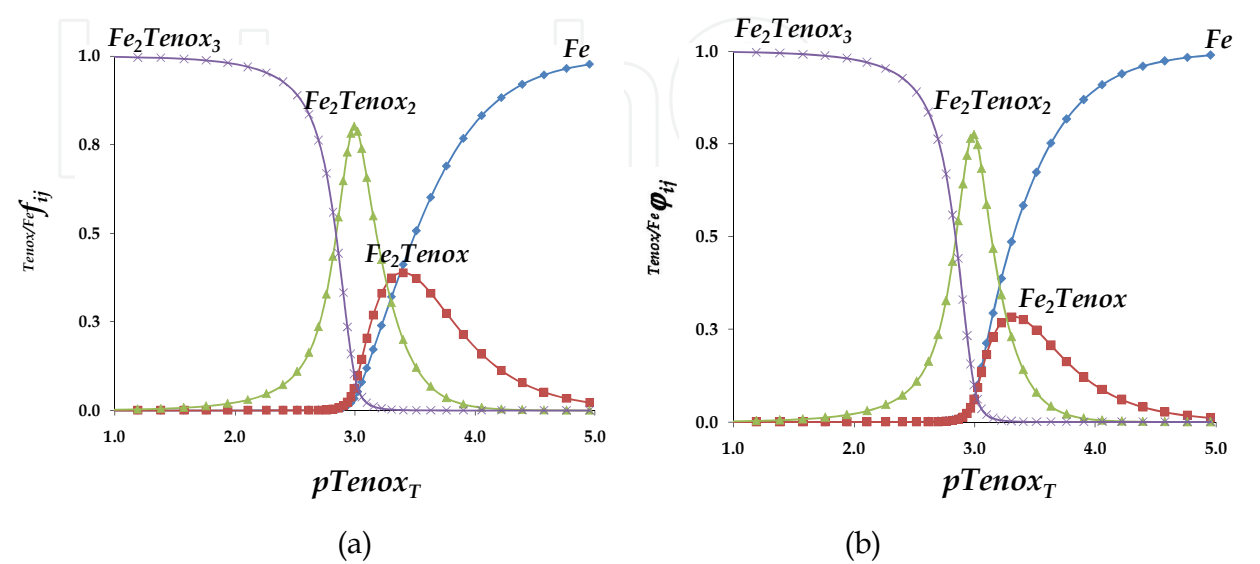

(a)   (b)

Fig. 2. Typical graphic representations of the Fe(III)-tenoxicam system in acetone as a function of p$Tenox_T$. $[Fe(III)]_T$ = 1×10^{-3} M and p$Tenox_T$ = -log$[Tenox]_T$. a) Distribution diagram of substance amount of Fe(III) species taking into account the quantity of Fe(III) in each species. b) Distribution diagram of concentration of Fe(III) species taking in account which Fe(III) species is more concentrated in the system.
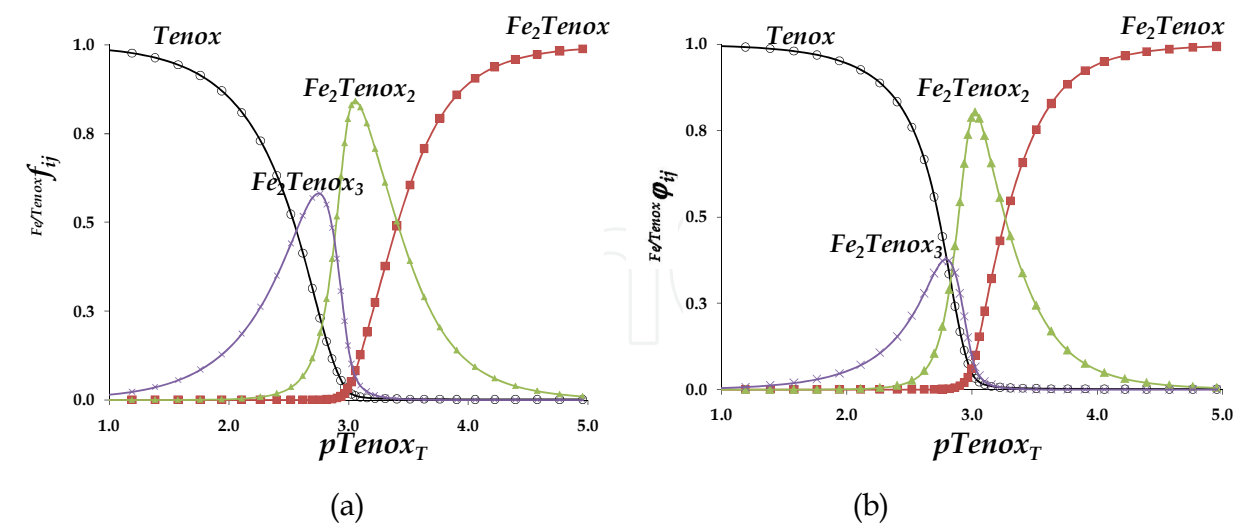

(a)   (b)

Fig. 3. Typical graphic representations of the Fe(III)-tenoxicam system in acetone as a function of p$Tenox_T$. $[Fe(III)]_T$ = 1×10^{-3} M and p$Tenox_T$ = -log$[Tenox]_T$. a) Distribution diagram of substance amount of Tenoxicam species, taking in account the quantity of tenoxicam in each species. b) Distribution diagram of concentration of tenoxicam species, taking in account which tenoxicam species is more concentrated in the system.

The independent variable of these figures, in all cases, has been selected to be the $pTenox_T$, in order to compare directly the shape of each fraction in Fig. 2 and 3. Nevertheless this axis could represent another variable (like $p\Sigma_M$, $p\Sigma_L$, pL, pM, etc.)

It is noteworthy than distribution of substance amount and concentration are similar for the same component, even though slightly differences can be shown comparing Fig. 2a and 2b, or Fig. 3a or 3b; some of their differences are crucial and related with the physical-chemical meaning of each distribution.

A distributions of Fe(III) and tenoxicam species comparison allows for the conclusion that they are very different, obviously representing distributions of two different components in the system.

2.2 Distribution diagrams as a function of stoichiometric coefficients

The sentence "distribution diagram" could have an implicit idea concerning possible statistical distributions subjacent to the graphic representations given in Fig. 1, 2 and 3. This idea was first explored by Moya-Hernández et al. (2002a) for the case of Brønsted acid-base systems. In the next subsection (2.2.1) the conclusions of this work will be applied to the case of oxine species as a function of pH while in the other subsection (2.2.2) this treatment will be generalized to the case of complex systems of the M-L kind, where polynuclear species are forming.

2.2.1 Distribution diagrams of one discrete variable (the proton stoichiometric coefficient for an acid-base system species)

If an aqueous solution of oxine at a certain concentration has a known pH value, the distribution of the oxine species will be fixed, as it is shown in Fig. 1a. Then a 3D graph could represent all the distributions of oxine species for each pH value. The set of distributions of oxine species is represented in Fig. 4 as well as one of them, at pH = 5.0.

In agreement with Mathematical Statistics (Kreyszig, 1970; Reichl, 1980), the meaning of each distribution of discrete variable is defined by Eq. 13.

$$\bar{v} = \sum_{j=0}^{n} j f_j \tag{13}$$

Furthermore, each of these statistical distributions has a variance. The variance of each distribution of discrete variable is defined by Eq. 14.

$$s_v^2 = \sum_{j=0}^{n} (j - \bar{v})^2 f_j \tag{14}$$

The equality of Eq. 3 and 13 demonstrate that the set of means of the oxine species distributions is the one given in Fig. 1b. In this way, the mean of the distribution offers the value in which the proton number is centered, as an average, at each pH value.

The set of variances of these distributions is related with an intrinsic buffer capacity (Moya-Hernández et al., 2002a). A graphic representation of the oxine set of variances as a function

of pH is given in Fig. 5. When the variance has a value near to zero one species is present in the system with a fraction near 1; when the variance reaches a maximum, two or more species are present in the system with comparable fraction values. In the case of oxine system the maxima of the variance function are reached for pH values equal to pK_{a1} and pK_{a2}, because $pK_{a2} \gg pK_{a1}$.
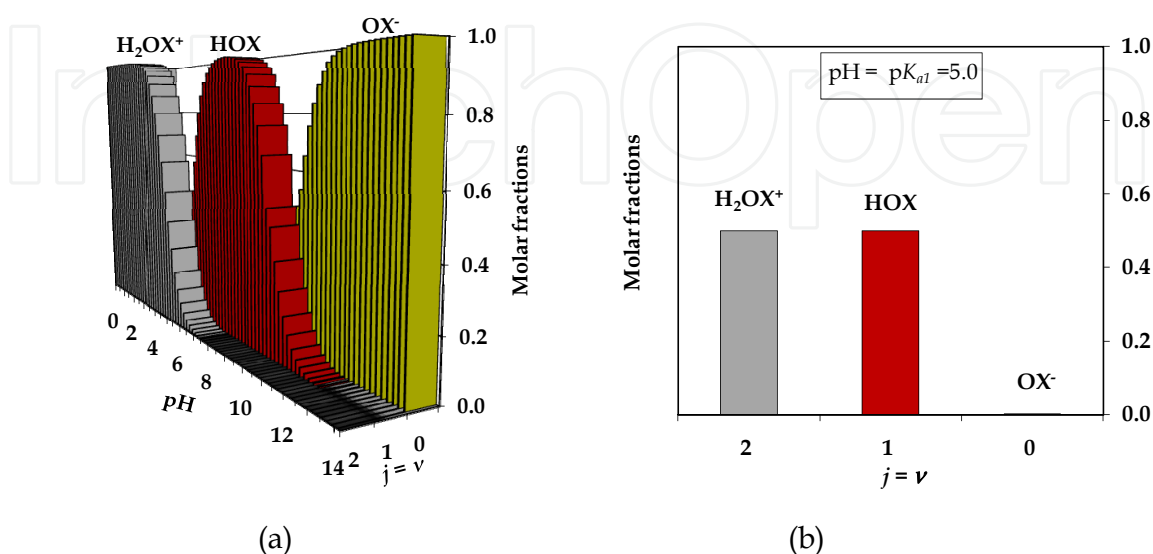

(a)   (b)

Fig. 4. Statistical distributions of oxine species. a) Set of distributions of the stoichiometric coefficient of protons as the discrete variable. b) Specific distribution diagram at pH = 5.0.
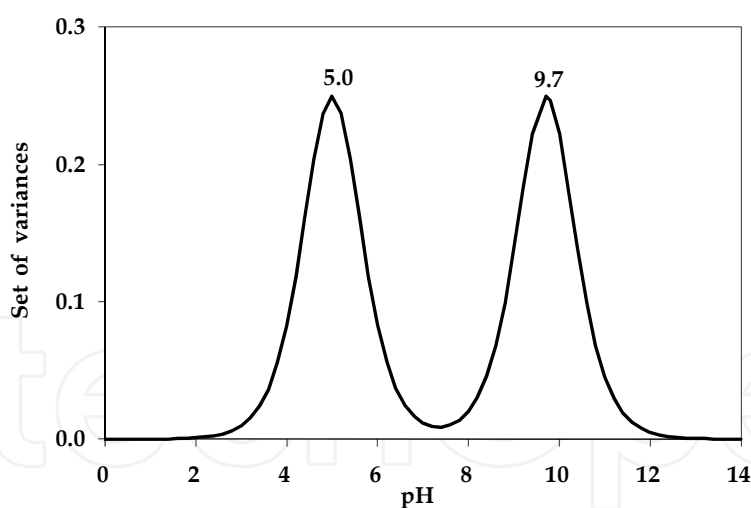

Fig. 5. Set of variances of the distributions of discrete variable of oxine as a function of pH. The maxima of these function are placed in the pK_a values.

2.2.2 Distribution diagrams of two discrete variables (the M and L components stoichiometric coefficients for complexation systems)

It can be demonstrated that the distribution diagrams as those of Fig. 2 and 3 for *M-L* complexation systems represent sets of distributions of two discrete variables,where these variables are the M and L stoichiometric coefficients.

Examples of substance amount and concentration distributions of tenoxicam in Fe(III), for only one of the systems represented in Fig. 2 are shown in Fig. 6.

In this case, each one of the statistical distributions that can be defined has two means, two variances and one covariance (Reichl, 1980).

Just as a mere example, the definition of the two means of the substance amount distribution of Tenoxicam in Fe(III) is given in Eq. 15, while the definition of the two variances and the covariance for the same distribution is given in Eq. 16.

$$
{}^{L/M}_{f}\overline{\nu}_M = \sum_{i=1}^{m}\sum_{j=0}^{n[i]}[i({}^{L/M}f_{ij})]
$$

$$
{}^{L/M}_{f}\overline{\nu}_L = \sum_{j=0}^{n}\sum_{i=1}^{m[j]}[j({}^{L/M}f_{ij})]
$$

(15)

(a)   (b)
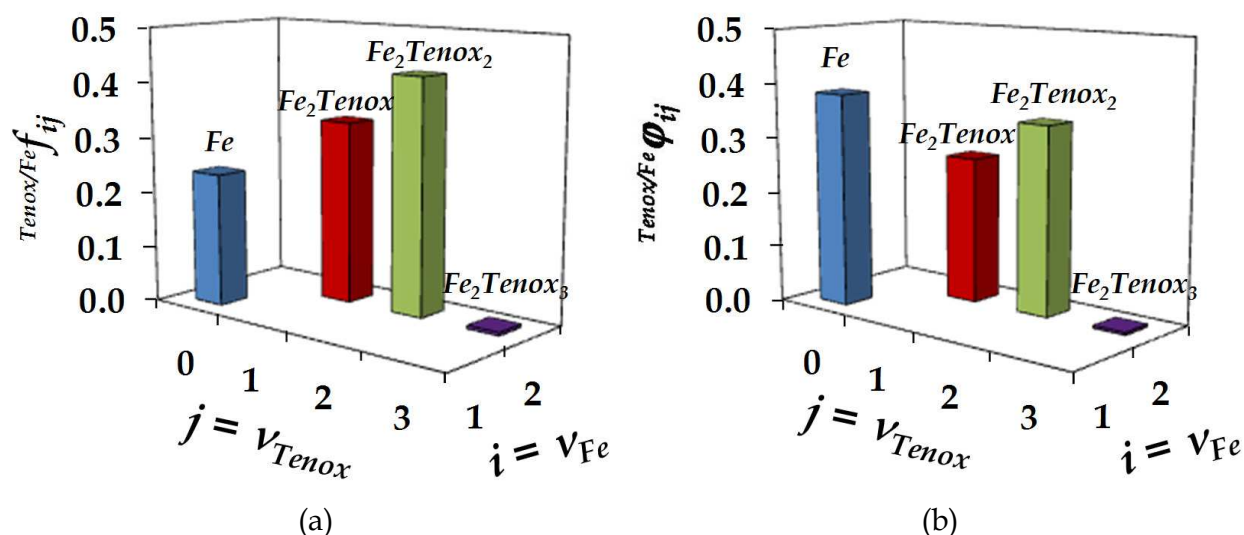
Fig. 6. Statistical distributions of tenoxicam in Fe(III) species in acetone. $[Fe(III)]_T = 1\times10^{-3}$M and $[Tenox]_T = 6\times10^{-4}$M. a) Substance amount fractions of Fe(III) species. b) Concentration fractions of Fe(III) species.

The set of means and variances for the distributions of two discrete variables of Tenoxicam in Fe(III), represented typically in Fig. 2a like a "distribution diagram", are shown in Fig. 7.

The interpretation of each of the two means is to be the stoichiometric coefficient average for the corresponding component. The two variances grow when two or more species are forming: higher variance increases the number of species with different stoichiometric coefficient of the corresponding component.

The possible consequences of this statistical view should be studied exhaustively, but this kind of study would be beyond the objectives of the present work. The distribution diagrams applications to determine or to use stoichiometric coefficients are developed in the following sections.

$$
{}^{L/M}_{f}S_{M,L} = \sum_{i=1}^{m}\sum_{j=0}^{n[i]}\{[i - ({}^{L/M}_{f}\bar{v}_M)]^2({}^{L/M}f_{M_iL_j})\}
$$

$$
{}^{L/M}_{f}S_{M,L} = \sum_{j=0}^{n}\sum_{i=1}^{m[j]}\{[j - ({}^{L/M}_{f}\bar{v}_L)]^2({}^{L/M}f_{ij})\} \tag{16}
$$

$$
{}^{L/M}_{f}S_{M,L} = \sum_{i=1}^{m}\sum_{j=0}^{n[i]}[(i - {}^{L/M}_{f}\bar{v}_M)(j - {}^{L/M}_{f}\bar{v}_L)({}^{L/M}f_{M_iL_j})]
$$

(a)   (b)
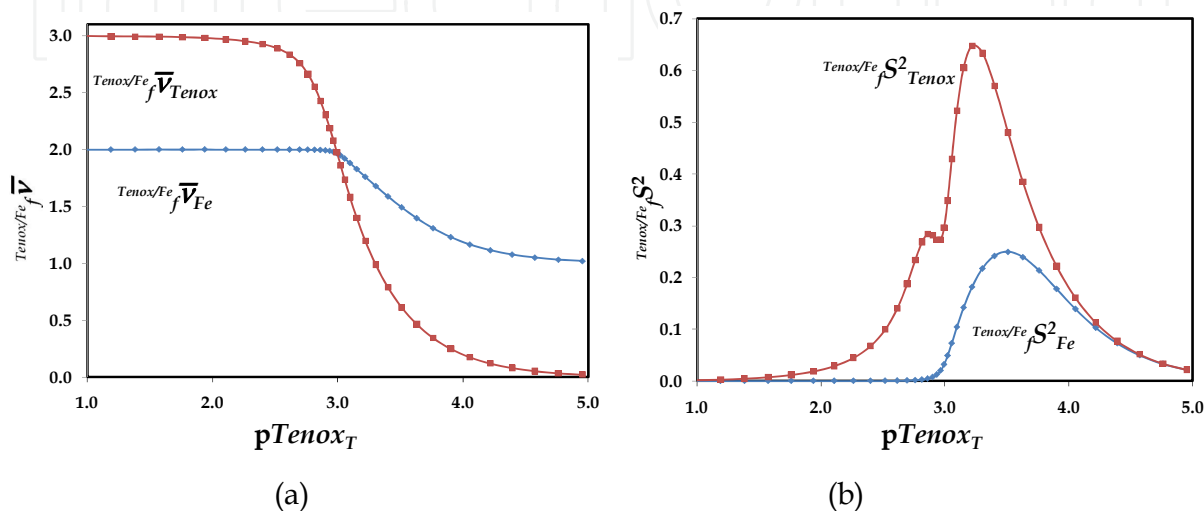
Fig. 7. Statistical parameters for the substance amount distributions of Tenoxicam in Fe(III) in acetone corresponding to Fig. 2a. a) Set of the two means of the distribution. b) Set of the two variances of the distribution.

3. Acid-base titration curves for polyprotic systems

This section deals with titration curves, pH = f(volume of strong acid or base), of polyacid and polybase systems by means of a description given by a thermodynamic model. This allows for the theoretical building of this kind of curves as well as their first derivative and the buffer capacity curves as a function of pH. The model is deducted from electroneutrality equation relating the global formation equilibrium and molar fractions of the distribution diagram of the system. Some previous works concerning this mater can be found in literature, by Fleck, 1967; Högfeldt, 1979; King & Kester, 1990; Efstathiou, 2000; Rojas-Hernández & Ramírez-Silva, 2002; Tarapčík & Beinrohr, 2003; Asuero, 2007; Gutz, 2010; Asuero & Michałowski, 2011.

3.1 Titration curves, pH = f(added volume of strong acid or base), of a mixture of species in the same polyprotic system

A system formed by a mixture of V_{oj} volumes of solutions of H_jL^{j-a} species, with concentrations C_{oj}, giving a total initial volume $V_o = \Sigma V_{oj}$, has been considered. The H_jL^{j-a} species form part of the same polyprotic system ($H_nL^{(n-a)+}/H_{(n-1)}L^{(n-a-1)+}/.../H_aL/.../HL^{(a-1)-}/L^{a-}/H^+$). Each charged species has associated a contra-cation or a contra-anion (M^{z+} or X^{z-}) that do not have acid-base properties, depending if ($j-a$) is negative or positive.

3.1.1 Titrations with a strong base: *MOH*

If the mixture described at the beginning of section 3.1 is titrated with a strong base *MOH*, of C_b concentration, it is possible to write the electroneutrality equation, for each added volume of *MOH* (V_b), in the form:

$$[M^+] + \frac{\sum_{j=0}^{a-1}(a-j)\{V_{oj}C_{oj}\}}{V_o+V_b} + \sum_{j=a+1}^{n}(j-a)[LH_j^{j-a}] + [H^+] =$$
$$= \frac{\sum_{j=a+1}^{n}(j-a)\{V_{oj}C_{oj}\}}{V_o+V_b} + \sum_{j=0}^{a-1}(a-j)[LH_j^{j-a}] + [OH^-] \tag{17}$$

where $[M^+] = V_bC_b/(V_o + V_b)$, the second term in the first member of Eq. 17, represents the contra-cations charge associated to the anions of the polyprotic system for $j \in \{0, 1, ..., a\text{-}1\}$, while the first term in the second member represents the contra-anions charge associated to the cations of the polyprotic system for $j \in \{a+1, a+2, ..., n\}$.

Introducing Eq. 1 and 2 in Eq. 17 and algebraically rearranging it, it is possible to arrive to Eq. 18.

$$V_b = \frac{\sum_{j=0}^{n}\{(j-a)(V_{oj}C_{oj})\} - \left[\sum_{j=0}^{n}(V_{oj}C_{oj})\right]\left[\sum_{j=0}^{n}\{(j-a)f_j\}\right] - V_o\left(\left[H^+\right] - \frac{K_w}{\left[H^+\right]}\right)}{C_b + \left[H^+\right] - \frac{K_w}{[H^+]}} \tag{18}$$

3.1.2 Titrations with a strong acid: *HX*

If the mixture described at the beginning of the section 3.1 is titrated with a strong acid *HX*, of C_a concentration, it is possible to write the electroneutrality equation, for each added volume of *HX* (V_a), in the form:

$$\frac{\sum_{j=0}^{a-1}(a-j)\{V_{oj}C_{oj}\}}{V_o+V_b} + \sum_{j=a+1}^{n}(j-a)[LH_j^{j-a}] + [H^+] =$$
$$= \frac{\sum_{j=a+1}^{n}(j-a)\{V_{oj}C_{oj}\}}{V_o+V_b} + \sum_{j=0}^{a-1}(a-j)[LH_j^{j-a}] + [OH^-] + [X^-] \tag{19}$$

where $[X^-] = V_aC_a/(V_o + V_a)$. Introducing Eq. 1 and 2 conveniently in Eq. 19 and algebraically rearranging it, it is possible to arrive to Eq. 20.
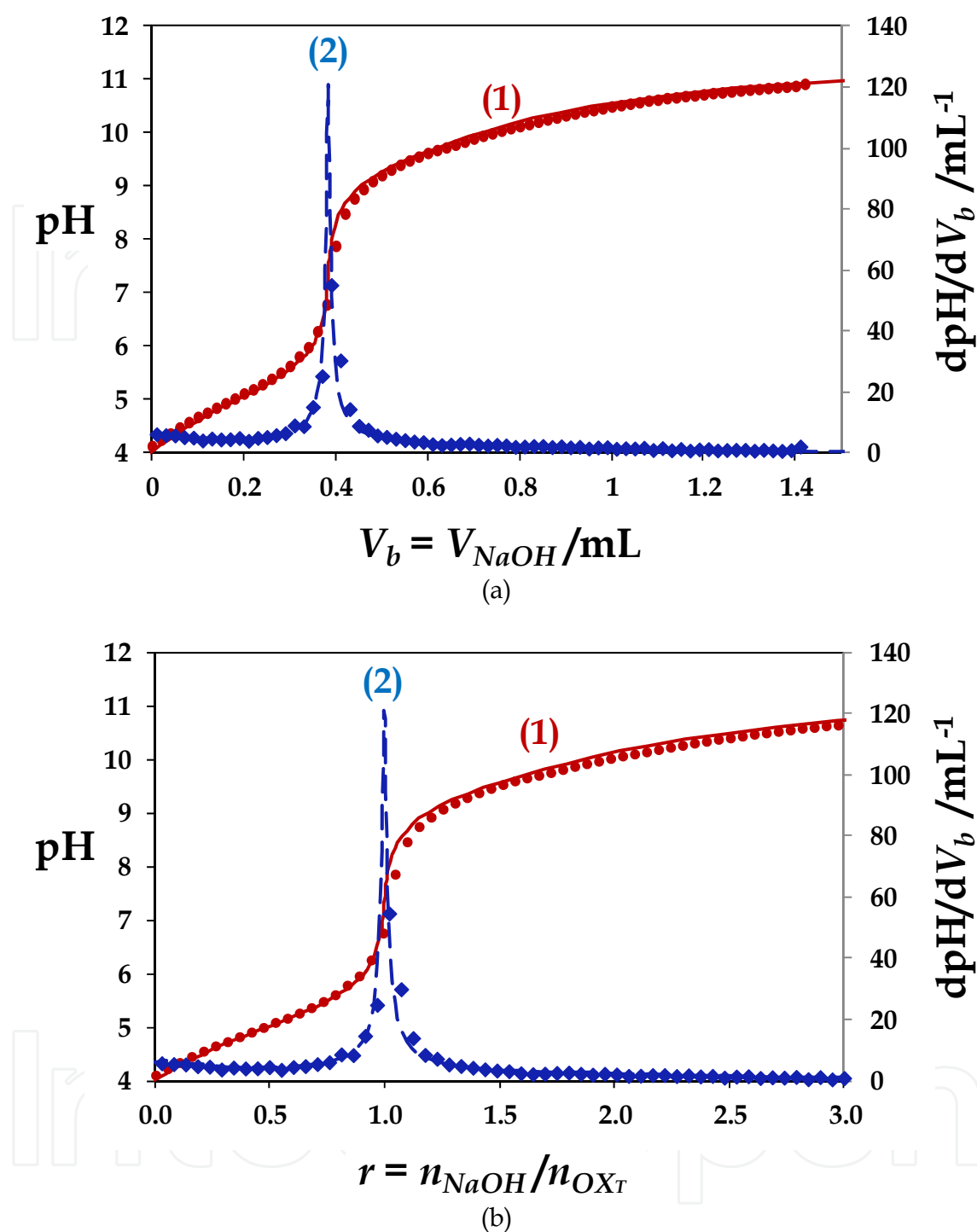
Fig. 8. Titration curve of 50 mL of aqueous solution of H_2OXCl with an aqueous solution of NaOH 0.1315 M. The values used to obtain the fitting shown are the following: pK_{a1} = 5.0, pK_{a2} = 9.7, pK_w = 13.7, $[H_2OXCl]_{initial}$ = 0.00101 M.
1) The circles represent the experimental points of the pH = f(V_b) curve and the solid line is the fitted curve obtained with Eq. 18. 2) The rhombuses represent the experimental points of the (dpH/dV_b) = g(V_b) curve and the dashed line is the fitted curve obtained with Eq. 22. a) Curves as a function of added volume of the titrand. b) Curves as a function of molar ratio (r) of the titrand.

Distribution Diagrams and Graphical Methods to Determine
or to Use the Stoichiometric Coefficients of Acid-Base and Complexation Reactions
299

Practically all the simulators, available nowadays, to predict acid-base titration curves, using strong base or acid as titrand agent, are based on Eq. 18 and 20. They are analytical expressions to calculate exactly the added volume of strong base or acid, given a set of pH values. In the following subsections this feature will be used to obtain important applications of these equations.

$$V_a = \frac{-\sum_{j=0}^{n}\{(j-a)(V_{oj}C_{oj})\} + \left[\sum_{j=0}^{n}(V_{oj}C_{oj})\right]\left[\sum_{j=0}^{n}\{(j-a)f_j\}\right] + V_o\left(\left[H^+\right] - \dfrac{K_w}{\left[H^+\right]}\right)}{C_b - \left[H^+\right] + \dfrac{K_w}{\left[H^+\right]}}$$

(20)

3.1.3 Titration of aqueous solution of oxine hydrochloride (H_2OXCl) with $NaOH$

In order to compare the predicted results with the experimental ones, 50 mL of an aqueous solution 0.001M H_2OXCl where titrated with a solution of NaOH 0.1315 M at 25°C.

The comparison of the experimental titration curve with the fitted curve through the model given by Eq. 18 is shown in Fig. 8a.

As it is shown in curves 1 of Fig. 8, the observed fitting for the titration curve is good. In the case of Fig. 8b, the molar ratio (r) is defined as the ratio of the added titrand (NaOH), with respect to the analyte (OX_T). The solution pH has a great change near 1, meaning that the quantitative reaction consumes 1 mol of H_2OX^+ for each added mol of OH^-. In other words, the stoichiometric coefficients of these reagents are 1 and 1 for the reaction that permits the quantification of oxine with the hydroxide ion:

$$H_2OX^+ + OH^- \rightleftharpoons HOX + H_2O$$

(21)
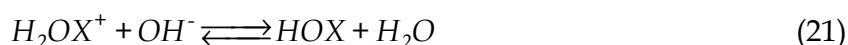
3.2 The first derivative of the titration curve: dpH/dV

The first derivative method of an acid-base titration curve is well known to determine the equivalence point volumes in order to accomplish quantitative chemical analysis.

Nevertheless, being Eq. 18 and 20 functions of only one variable (the pH), it is possible to obtain the analytical expressions of their first derivatives and their reciprocal functions, to arrive to the exact algebraic expressions of the titration first derivatives curves. These expressions are given in Eq. 22 and 23.

$$\frac{dpH}{dV_b} = \frac{C_b + 10^{-pH} - 10^{pH-pK_w}}{-2.303\left[\sum_{j=0}^{n}(V_{oj}C_{oj})\right]\left[\sum_{j=0}^{n}\left\{jf_j\sum_{i=0}^{n}[(i-j)f_i]\right\}\right] + 2.303(V_o + V_b)\left[10^{-pH} + 10^{pH-pK_w}\right]}$$

(22)

$$-\frac{dpH}{dV_a} = \frac{C_a - 10^{-pH} + 10^{pH-pK_w}}{-2.303\left[\sum_{j=0}^{n}(V_{oj}C_{oj})\right]\left[\sum_{j=0}^{n}\left\{jf_j\sum_{i=0}^{n}[(i-j)f_i]\right\}\right] + 2.303(V_o + V_a)\left[10^{-pH} + 10^{pH-pK_w}\right]}$$

(23)

3.2.1 Titration first derivative curve of an oxine hydrochloride (*H₂OXCl*) aqueous solution with *NaOH*

The curves 2 in Fig. 8 compare the titration experimental first derivative, described at the beginning of subsection 3.1.3, with the curves obtained by Eq. 22.

The experimental first derivative was obtained approximately as the ratio of finite differences of measured pH values and volumes during titration, using the average of volumes, or molar ratios, for each interval.

As it can be seen, the fitting attained is quite good and the maximum observed in Fig. 8a and 8b is sharp. In the first case, this maximum signals the volume position of the first equivalence point, while in the second case it indicates the ratio of the titrand stoichiometric coefficients with respect to the analyte for the quantitative reaction.

The first derivative is usually better than the pH curve to experimentally determine the volumes of the equivalence points (Fig. 8a) and the titration reactions (titrand/analyte) ratio of stoichometric coefficients (Fig. 8b) when these are quantitative.

In the case of the *HOX* reaction with OH^-, the second titration reaction, is not quantitative because its corresponding equilibrium constant is not high enough for a 0.001 M analyte initial concentration. For this reason there are no visible changes in the second equivalence point volume in curves 1 or 2 in Fig. 8a, nor in Fig. 8b for $r = 2$.

3.3 The buffer capacity (β) of a polyprotic system

In many chemical and biological processes it is essential that the medium pH be kept within certain limits, which is possible through the use of buffer solutions. They possess a specific buffer capacity and are used to maintain constant the pH with a very small uncertainty.

In the chemical literature, there are two ways to define a buffer capacity (**β**): one is defined in terms of concentration of strong acid or base added to the system, in order to simplify the mathematical treatment, as firstly proposed by Van Slyke (1922), and then used by others, as Urbansky & Schock (2000) or Segurado (2003). The other way to define the buffer capacity is in terms of the amount of strong acid or base added to the system, as King and Kester did (1990), as well as Skoog et al. (2005); they also derive equations with the concentration, but considering explicitly 1L of solution.

3.3.1 A buffer capacity with dilution effect (β$_{dil}$)

According to the definition given by King & Kester (1990) it is possible to apply the derivative of the added amount of strong base or acid with respect to the pH, and then obtaining mathematical expressions for the buffer capacity as function of pH, by considering the dilution effect, i.e. **β$_{dil}$** = f(pH). In the present work, this implies to take Eq. 22 and 23 reciprocals and multiply them by C_b or C_a, respectively.

The typical way to represent a buffer capacity curve, consists in plotting it as a function of pH, even though it may be represented as a function of the titrand volume or the molar ratio titrand/analyte.

$$\beta_{\text{dil }b} = \frac{dV_b C_b}{dpH} = \frac{2.303 C_b}{C_b + (10^{-pH} - 10^{pH - pK_w})}$$
$$\left\{ \left[\sum_{j=0}^{n} (V_{oj} C_{oj}) \right] \left[-\sum_{j=0}^{n} \left(jf_j \sum_{i=0}^{n} [(i-j) f_i] \right) \right] + (V_o + V_b) \left[10^{-pH} + 10^{pH - pK_w} \right] \right\}$$

(24)

$$\beta_{\text{dil }a} = -\frac{dV_a C_a}{dpH} = \frac{2.303 C_a}{C_a - (10^{-pH} - 10^{pH - pK_w})}$$
$$\left\{ \left[\sum_{j=0}^{n} (V_{oj} C_{oj}) \right] \left[-\sum_{j=0}^{n} \left(jf_j \sum_{i=0}^{n} [(i-j) f_i] \right) \right] + (V_o + V_a) \left[10^{-pH} + 10^{pH - pK_w} \right] \right\}$$

(25)

As Moya-Hernández et al. (2002b) have demonstrated, Eq. 14 is equal to the double sum between brackets in Eq. 24 and 25. For this reason, the set of variances is related with the intrinsic buffer capacity of a polyprotic system.

$$s_\nu^2 = \sum_{j=0}^{n} (j - \bar{\nu})^2 f_j = \left[-\sum_{j=0}^{n} \left(jf_j \sum_{i=0}^{n} [(i-j) f_i] \right) \right] = intrinsic\ buffer\ capacity$$

(26)

It is noteworthy that the intrinsic buffer capacity, i.e. the set of variances of the proton stoichiometric coefficient distributions for this kind of systems, is a function that only depends on the molar fractions and the stoichiometric coefficients.

The second term between keys in Eq. 24 and 25 is due to the acid and basic particles of the amphiprotic solvent (H⁺ and OH^- in the case of water). (See Segurado (2003), Urbansky & Schock (2000).)

3.3.2 Buffer capacity with dilution of aqueous solution of oxine hydrochloride (H_2OXCl) with $NaOH$

Fig. 9 shows the comparison of experimental buffer capacity, with effect of dilution, and the curve obtained by Eq. 24 and 25 for the titrations of the system defined at the beginning of subsection 3.1.3.
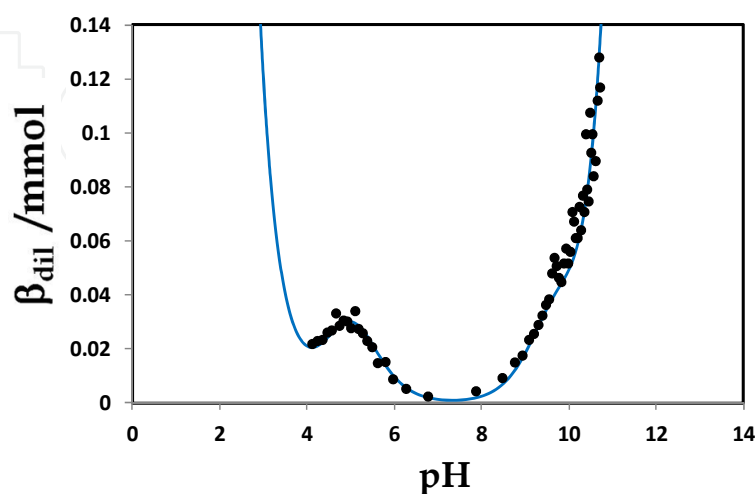

Fig. 9. Comparison of experimental (markers) and calculated (solid line) buffer capacity with effect of dilution.

The experimental β_{dil} has been determined approximately by taking the ratio of the titrand concentration and the first derivative experimentally obtained as explained in subsection 3.2.1.

As it can be seen in Fig. 9, there is a good agreement between the theoretical and the experimental data. The expected maximum of the curve at pH = pK_{a2} = 9.7 (see Fig. 5) is lost due to the effect of the hydroxide ion over the pair HOX/OX^- by the low concentration of oxine in the system (0.001 M).

4. Molar ratio and continuous variations methods for complexation systems

For complexation reactions the two traditional methods to determine the stoichiometry of formation reactions and formation equilibrium constants are the molar ratio and the continuous variations methods (this last also known as Job's method). (See Hartley et al., 1980.)

Nevertheless, the explanation of these methods has not always been given in a clear way, and this is particularly evident for equilibrium considering the formation of polynuclear species. Furthermore, these treatments are disappearing from modern text books. For this reason, the aim of this part of the chapter is to describe a way to deduct the equations and the curves that appear in some Inorganic and Analytical Chemistry books.

4.1 Tables of Variation of Substance Amount (TVSA)

Professor Gaston Charlot (1969), in France, has used a teaching tool to explain the advance degree in the formation of acid-base, complexation and redox reactions. It has been called by him the Table of Variation of Substance Amount. In the following subsections this tool will be applied to the systems equilibrium states using the molar ratio and continuous variations methods.

For a system where only one reaction takes place, quantitatively:

$$aM + bL \rightleftharpoons M_aL_b \quad \text{with} \quad \beta_{ab} = \frac{[M_aL_b]}{[M]^a [L]^b} >> 1 \qquad (27)$$
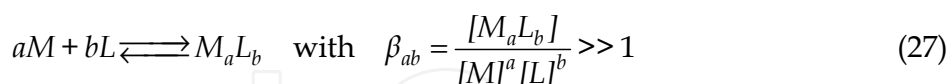
4.1.1 Table of Variation of Substance Amount for the molar ratio method

In the molar ratio method several amounts of one of the reagents, i. e. L, is added to another reagent, i. e. M, and typically the dilution of the solutions is controlled in volumetric flasks of the same capacity V_T in order to measure a response R that is directly proportional to the reaction product, M_aL_b, through the equation:

$$R = k_{M_aL_b}[M_aL_b] = k_{M_aL_b}(n_{M_aL_b} / V_T) \qquad (28)$$

This experiment is described in Table 2 for a quantitative reaction.

If all the amounts in the first column of Table 2 are divided by the M quantity (n_M), and the amounts in the other columns are divided by V_T and multiplied by the corresponding response factor, Table 3 will be obtained.

Initial	$a\,M$ n_M	$+$	$b\,L$ n_L	$\leftrightarrows$	M_aL_b
$n_L < \dfrac{b}{a} n_M$	$n_M - (a/b)n_L$		$b\epsilon \approx 0$		$(1/b)n_L$
$\dfrac{b}{a} n_M = {}_{SC}n_L$	$a\epsilon \approx 0$		$b\epsilon \approx 0$		$(1/a)n_M$
$\dfrac{b}{a} n_M < n_L$	$a\epsilon \approx 0$		$n_L - (b/a)n_M$		$(1/a)n_M$

Table 2. TVSA for molar ratio method. n_M is a constant for all the systems, n_L is variable, all systems are in solution in thermodynamic equilibrium and the total volume is the same and equal to V_T. ${}_{SC}n_L$ represents the amount of L for the stoichiometric condition.

The functions deducted for molar ratio method and presented in Table 3, with the given restrictions, lead to represent their behaviour in Fig. 10 assuming Eq. 28 and giving R in arbitrary units.

Initial	$a\,M$ n_M	$+$	$b\,L$ n_L	$\leftrightarrows$	M_aL_b
$r_L < \dfrac{b}{a}$	$k_M(n_M - (a/b)n_L)/V_T$		$b\epsilon \approx 0$		$k_{MaLb}(1/b)r_L(n_M)/V_T$
${}_{SC}r_L = \dfrac{b}{a}$	$a\epsilon \approx 0$		$b\epsilon \approx 0$		$k_{MaLb}(1/a)n_M/V_T$
$\dfrac{b}{a} < r_L$	$a\epsilon \approx 0$		$k_L(n_L - (b/a)n_M)/V_T$		$k_{MaLb}(1/a)n_M/V_T$

Table 3. TVSA for molar ratio method expressed in terms of molar ratio of L (r_L) and response (R) of the system. ${}_{SC}r_L$ represents the amount of L for the stoichiometric condition. For this study it has been assumed that $k_M = k_L = 0$.

It should be noticed in Fig. 10 that the intersection between the two formed straight lines indicates the molar ratio corresponding to stoichiometric conditions; in other words, this value is equal to the L stoichiometric coefficient ratio divided by the M stoichiometric coefficient : ${}_{SC}r_L = b/a$.
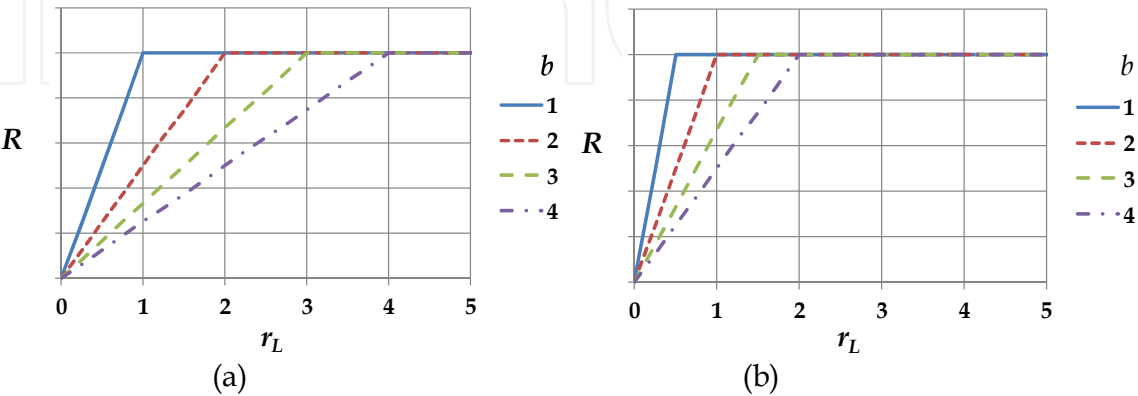

Fig. 10. Curves *Response* $= R= f(r_L)$ for experiments of molar ratio method. a) $a = 1$ for the formation of species of the ML_b kind. b) $a = 2$ for the formation of species of the M_2L_b kind.

If some of the assumptions formulated in this work are avoided there will be some deviations of the curves shown in Fig. 10. As an example, if more species linearly contribute to the response, the parameters of the straight lines change, but their intersection still indicates the molar ratio of the stiochiometric conditions. If the formation reaction in Eq. 27 is not quantitative there will be some deviations of the linearity near the stoichiometric conditions. Finally, if there are more species forming in the system at the same time, in principle, there will be more straight lines in the molar ratio curve, one for each species appearing in the system (if all the reactions are quantitative, if all the contributions to the response are linear and the response factors are different enough).

4.1.2 Tables of Variation of Substance Amount for the continuous variations method

In the continuous variations method several amounts of the reagents, L and M, are mixed in such a way that the total amount of both reagents is constant: $n_M + n_L = n_T$ = constant. Typically, the solutions dilution is controlled in volumetric flasks of the same capacity V_T in order to measure a response R that is directly proportional to the reaction product, M_aL_b, through Eq. 28. This experiment is described in Table 4 for a quantitative reaction.

Generally, in this method the equilibrium conditions are expressed in terms of the molar fraction of one of the components, x_L or x_M. So the $_{SC}x_L$ (the component L molar fraction at stoichiometric conditions) can be deduced, as it is shown in Eq. 29.

$$\frac{b}{a} = \frac{_{SC}n_L}{n_T - _{SC}n_L} \Rightarrow \frac{b}{a}(n_T - _{SC}n_L) = _{SC}n_L$$

$$\Rightarrow _{SC}x_L = \frac{b}{a}(1 - _{SC}x_L) \Rightarrow _{SC}x_L = \frac{\dfrac{b}{a}}{1+\dfrac{b}{a}} \qquad (29)$$

$$\therefore _{SC}x_L = \frac{b}{a+b}$$

$n_M + n_L = n_T$	$a\,M$	$+$	$b\,L$	$\leftrightarrows$	M_aL_b
Initial	$n_T - n_L$		n_L		
$n_L < {}_{SC}n_L$	$n_T - n_L - (a/b)n_L$		$b\epsilon \approx 0$		$(1/b)n_L$
$n_L = {}_{SC}n_L$	$a\epsilon \approx 0$		$b\epsilon \approx 0$		$(1/b)({}_{SC}n_L)$
${}_{SC}n_L < n_L$	$a\epsilon \approx 0$		$n_L - (b/a)(n_T - n_L)$		$(1/a)(n_T - n_L)$

Table 4. TVSA for continuous variations method. n_T is a constant for all the systems, n_M and n_L are variable, all systems are in solution in thermodynamic equilibrium and the total volume is the same and equal to V_T. $_{SC}n_L$ represents the amount of substance of L for the stoichiometric condition.

If all the amounts in the first column of Table 4 are divided by n_T, while the amounts in the other columns are divided by V_T and multiplied by the corresponding response factor, Table 5 will be obtained.

The functions deduced for continuous variations method and presented in Table 5, with the given restrictions, lead to represent their behaviour in Fig. 11 assuming Eq. 28 and giving R in arbitrary units.

Distribution Diagrams and Graphical Methods to Determine
or to Use the Stoichiometric Coefficients of Acid-Base and Complexation Reactions
305

$x_M + x_L = 1$	$a\,M$	+	$b\,L$	$\leftrightarrows$	M_aL_b
Initial	$n_T - n_L$		n_L		
$0 \le x_L \le \dfrac{b}{a+b}$	$k_M(n_T-((b-a)/b)n_L)/V_T$		$b\epsilon \approx 0$		$(k_{MaLb}/b)x_Ln_T/V_T$
$\dfrac{b}{a+b} = {}_{SC}x_L$	$a\epsilon \approx 0$		$b\epsilon \approx 0$		$(k_{MaLb}/(a+b))n_T/V_T$
$\dfrac{b}{a+b} \le x_L \le 1$	$a\epsilon \approx 0$		$k_L(n_L-(b/a)(n_T-n_L))/V_T$		$(k_{MaLb}/a)(1-x_L)n_T/V_T$

Table 5. TVSA for continuous variations method expressed in terms of L molar fraction (x_L) and response (R) of the system. $_{SC}x_L$ represents the amount of L substance for the stoichiometric condition. For this study it has been assumed that $k_M = k_L = 0$.

It should be remarked in Fig. 11 that the intersection between the two formed straight lines indicates the molar fraction corresponding to stoichiometric conditions; in other words, this molar fraction is equal to the following relationship: $_{SC}x_L = b/(a+b)$.

Moreover, in this method, as it has been discussed for the molar ratio method, if some of the assumptions formulated in this work are avoided there will be some deviations of the curves shown in Fig. 11. As an example, if more species contribute to the response, the parameters of the straight line change, but their intersection still indicates the molar fraction of the stiochiometric conditions. If the formation reaction in Eq. 27 is not quantitative, there will be some deviations of the linearity near the stoichiometric conditions. Finally, if there are more species forming in the system at the same time, in principle, there will be more straight lines in the molar ratio curve, one for each species appearing in the system (if all the reactions are quantitative, if all the contributions to the response are linear and the response factors are different enough).
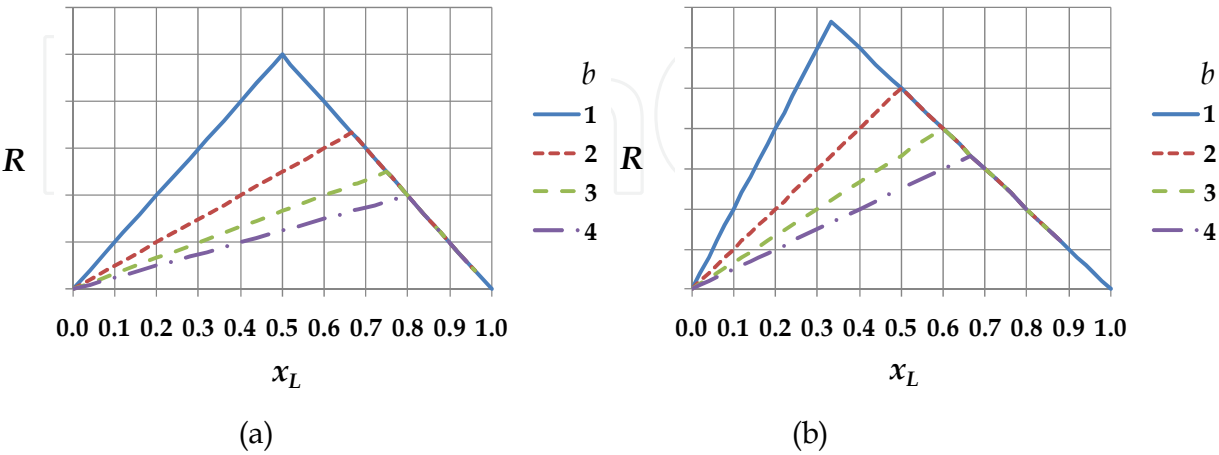

Fig. 11. Curves *Response* = R = f(x_L) for experiments of continuous variations method. a) $a = 1$ for the formation of species of the ML_b kind. b) $a = 2$ for the formation of species of the M_2L_b kind.

4.1.3 Some remarks for the use of Tables of Variation of Substance Amount

The TVSA are a very powerful tool to understand the composition of thermodynamic equilibrium states when chemical reactions are involved. In the subsections 4.1.1 and 4.1.2 the dependent and independent variables are those typically selected. Nevertheless other selections could be used if the description and interpretation of chemical behaviour require it. Then, in the molar ratio method the representation of the curves could be done as a function of metal ion ratio (r_M), while for the continuous variations method the molar fraction of metal ion (x_M) could be used.

Furthermore, the TVSA could be used for the treatment of several complexes forming in the system at the same time.

In this work we have presented only the curves that may help interpreting the system that will be treated in the following section.

4.2 Application of the methods to determine the stoichiometry and equilibrium constants: The case of Fe(III)-tenoxicam system in acetone

A spectroscopic study in the visible region of electromagnetic spectrum was undertaken to determine the complexes formed as well as their formation constants for the Fe(III)-tenoxicam system in acetone, due to the red colour observed when both reagents are mixed. The solutions preparation and the details of the spectra acquisition have been given elsewhere (Moya-Hernández et al., 2009).

The absorption spectra obtained in this study are presented in Fig. 12, for molar ratio and continuous variations methods.

In order to be near the fulfilment of the conditions selected in section 4.1, (e.g. absorption only due to the complexes formed) a wavelength of 520 nm was selected to represent the typical curves of molar ratio and continuous variations, which are shown in Figure 13.

(a)   (b)
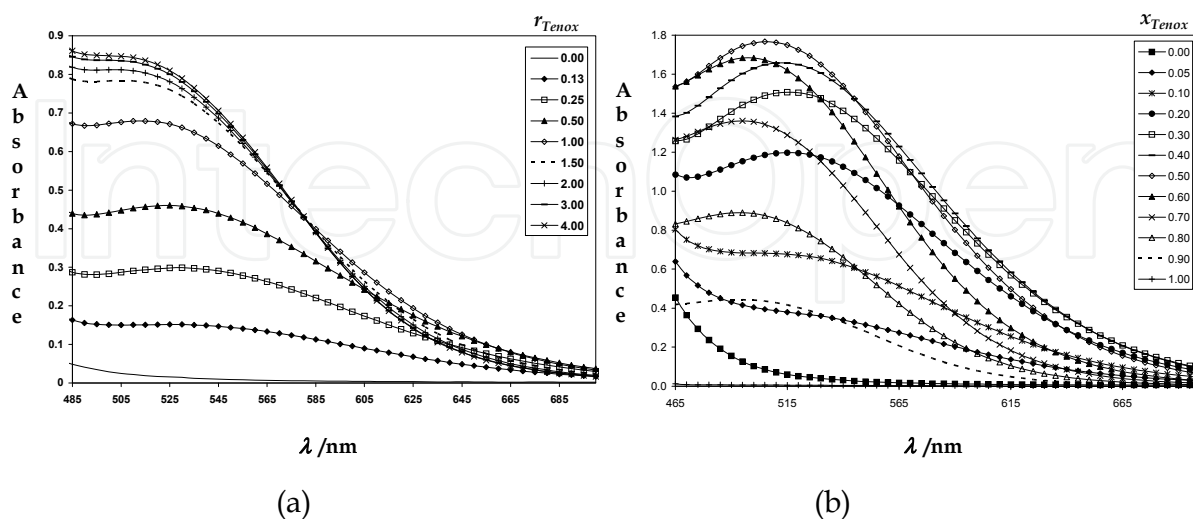
Fig. 12. Absorption spectra in the visible region for the Fe(III)-tenoxicam system in acetone. [Fe(III)] = 0.001M or [Fe(III)] + [Tenox] = 0.001M. a) Molar ratio method. b) Continuous variations method.
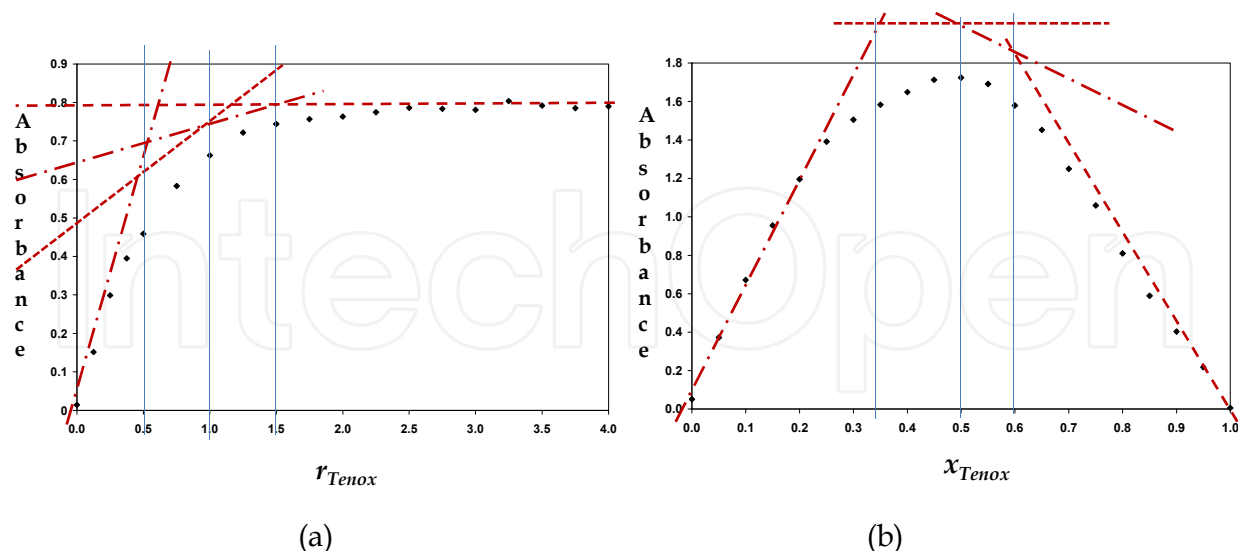
(a) (b)

Fig. 13. Spectral behaviour, at 520 nm, of the Fe(III)-tenoxicam system in acetone where different complexes are forming. [Fe(III)] = 0.001M or [Fe(III)] + [Tenox] = 0.001M. a) Molar ratio method. b) Continuous variations method. The dashed lines and the thin vertical lines only have been added to help follow the discussion given in the text.

The shape of the curves presented in Fig. 13 demonstrates the formation of polynuclear species in the system, both methods clearly showing an abrupt change of slope before the molar ratio or molar fraction corresponding to 1:1 stoichiometry (r_{Tenox} < 1 and x_{Tenox} < 0.5), as it can be concluded form Fig. 10b and 11b. The other changes in slope support the possibility of the formation of several complexes; in other words, two straight lines are not enough to explain the shape of the curves. The thin vertical lines indicate the position of the molar ratio or the molar fraction that fulfil the stoichiometric conditions of the Fe(III)-tenoxicam complexes (*Fe₂Tenox*, *Fe₂Tenox₂* and *Fe₂Tenox₃*) obtained in the treatment of spectrophotometric data (Moya-Hernández et al., 2009 and Table 1).

In order to better describe the physical-chemical behaviour observed in the molar ratio method, the distribution diagrams of discrete variable of tenoxicam in Fe(III) (for the concentration of Fe(III) species) for the thin vertical lines shown in Fig. 13a, are presented in Fig. 14.

As it can be seen in Fig. 14, the predominant complex in the system corresponds to the molar ratio of each system, with other Fe(III) species been important as well. This is the reason why the experimental points are placed outside straight (dashed) lines in Fig. 13a.

Although some of these distribution diagrams of discrete variable could be represented for the continuous variations method, Fig. 13b may be the best graphic representation could be a distribution that consider Fe(III) and tenoxicam species at the same time, being the sum of substance amount of Fe(III) and tenoxicam (n_{Fe} +n_{Tenox} = n_T = constant) the biggest restriction of this method. A look of this kind of distributions have been previously developed (Moya-Hernández, 2003).
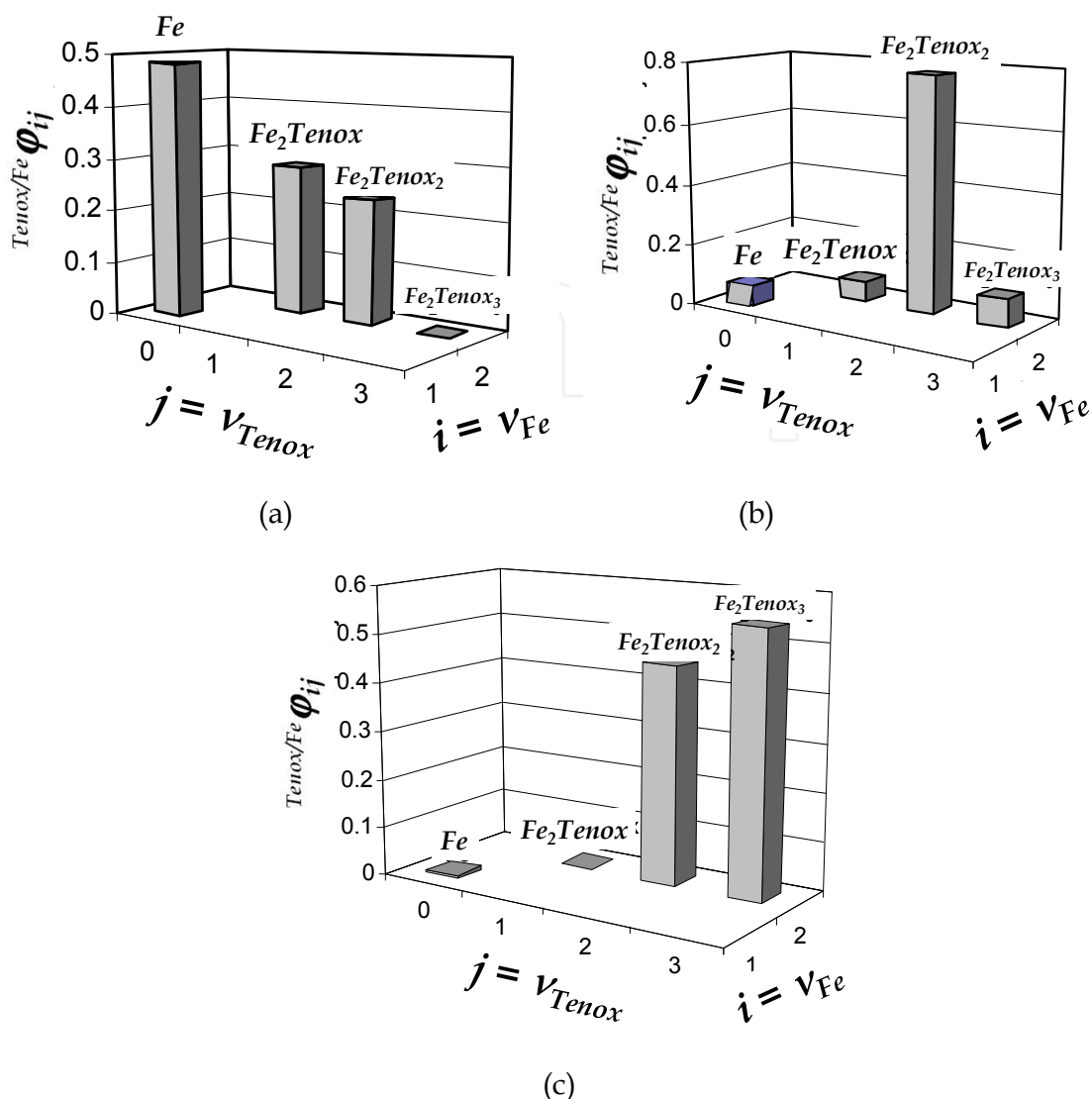
(a)

(b)

(c)

Fig. 14. Distribution diagrams of concentration of tenoxicam in Fe(III), for Fe(III) species, of some of the systems related with Fig. 13a. a) $r_{Tenox} = 0.5$. b) $r_{Tenox} = 1.0$. c) $r_{Tenox} = 1.5$.

5. Conclusion

In this work, some novelties related with the distribution diagrams, understood as statistical distributions of discrete variables, have been presented. We have extended this vision for two component systems. Moreover, the fractions of the distribution diagrams have been used to develop analytical equations to calculate exactly pH-metric titration curves as well as their first derivatives and a buffer capacity with effect of dilution. Finally the molar ratio and continuous variations methods have been reviewed, according to Charlot's methods, and explained with the discrete variables statistical distributions for complexation systems.

6. Acknowledgments

7. References

Asuero, A. G. Buffer Capacity of a Polyprotic Acid: First Derivative of the Buffer Capacity and pK_a Values of Single and Overlapping Equilibria. *Critical Reviews in Analytical Chemistry*, Vol.37, (July 2007), pp. 269-301.

Asuero, A. G. & Michałowski, T. Comprehensive Formulation of Titration Curves for Complex Acid-Base Systems and Its Analytical Implications. *Critical Reviews in Analytical Chemistry*, Vol.41, (May 2011), pp. 151-187.

Charlot, G. (1969). Cours de Chimie Analytique Générale, Vol.1. Solutions Aqueuses et Non Aqueuses, Masson, Paris, France

Efstathiou, C. E. (2000). Acid-base titration curves, Applet, Department of Chemistry, University of Athens, Greece, Available from
    http://www.chem.uoa.gr/Applets/AppletTitration/Appl_Titration2.html

Fleck, G. M. (1967). *Equilibrios en Disolución,* Alhambra, Madrid, Spain

Gutz, I. G. R. (September 2011). Simulator: CurTiPot. Version 3.5.4, MS Excel. Institute of Chemistry, University of Sao Paulo, Brazil. Available from
    http://www2.iq.usp.br/docente/gutz/Curtipot_.html

Hartley, F. R., Burgess, C. & Alcock R. M. (1980). *Solution Equilibria*, Ellis Horwood, Chichester, UK

Högfeldt, E. (1979). Chapter 15, In: *Treatise on Analytical Chemistry*, Kolthoff, I. M., Elving, P. J. Part 1, Vol.2, Section D, Interscience, ISBN: 978-047-1055-10-5, New York, USA

King, D. W.; Kester, D. R. (1990). A General Approach for Calculating Polyprotic Acid Speciation and Buffer Capacity. *Journal of Chemical Education*, Vol.67, No. 11, pp. 932-933.

Kreyszig, E. (1970). *Introductory Mathematical Statistics: Principles and Methods*, Wiley, New York, USA

Moya-Hernández, R.; Rueda-Jackson, J. C.; Ramírez-Silva, M. T.; Vázquez-Coutiño, G. A.; Havel, J. & Rojas-Hernández, A. (2002a). Statistical Study of Distribution Diagrams for Two-component Systems: Relationships of Means and Variances of the Discrete Variable Distributions with Average Ligand Number and Intrinsic Buffer Capacity. *Journal of Chemical Education*, Vol.79, No.3, (March 2002), pp. 389-392.

Moya-Hernández, R.; Rueda-Jackson, J. C.; Ramírez-Silva, M. T.; Vázquez-Coutiño, G. A.; Havel, J. & Rojas-Hernández, A. (2002b). Statistical Study of Distribution Diagrams for Two-component Systems: Relationships of Means and Variances of the Discrete Variable Distributions with Average Ligand Number and Intrinsic Buffer Capacity. *Journal of Chemical Education*, Vol.79, No.3, (March 2002), pp. 389-392. Supplemental Material for Journal of Chemical Education On Line, Available form
    http://jchemed.chem.wisc.edu/Journal/Issues/2002/Mar/PlusSub/JCESupp/supp389.html

Moya-Hernández, R. (2003). Estudio de Especiación Química de los Fármacos Antiinflamatorios Tenoxicam y Piroxicam con Cationes Metálicos de Interés Biológico, Ph. D. Thesis, Universidad Autónoma Metropolitana, Unidad Iztapalapa, México, D. F., Mexico.

Moya-Hernández, R., Gómez-Balderas R., Mederos A., Domínguez S., Ramírez-Silva M. T. & Rojas-Hernández A. (2009). *Journal of Coordination Chemistry*, Vol.62, No.1, pp. 40-51.

Puigdomenech, I. (May 2011). Make Equilibrium Diagrams Using Sophisticated Algorithms (MEDUSA), Available from http//www.kemi.kth.se/medusa

Reichl, L. E. (1980). A *Modern Course in Statistical Physics*, University of Texas Press, Austin, USA

Ringbom, A. (1963). *Complexation in Analytical Chemistry*, Wiley, New York, USA

Rojas-Hernández, A.; Ramírez, M. T.; González, I. & Ibanez, J. G. Predominance-Zone Diagrams in Solution Chemistry. Dismutation Processes in Two-Component Systems (M-L). *Journal of Chemical Education*, Vol.72, No.12, (December 1995), pp. 1099-1105

Rojas-Hernández, A. & Ramírez-Silva M. T. (2002). Modelo Termodinámico General para Curvas de Valoración Ácido-Base de Mezclas de Sistemas Poliácidos o Polibásicos (Sin Polinucleación) Con Ácido o Base Fuertes, In: *Química Inorgánica en la UAM-Iztapalapa 2002*, López-Goerne, T. M. & Rojas-Hernández, A. Vol. 1. pp. 133-158, ISBN: 970-31-0149-6, México, D. F., Mexico

Segurado, M. A. P. (2003). Extreme Values in Chemistry: Buffer capacity. *Chemical Educator*, Vol.8, pp. 22-27

Skoog, D. A. West, D. M., Holler, F. J. & Crouch, S. R. (2004). Fundamentals of Analytical Chemistry, 8th Ed., Brooks/Cole, Thompson Learning, Belmont, USA

Tarapčík, P., & Beinrohr, E. (2003). Implementation of a Universal Algorithm for pH Calculation into Spreadsheet and its Use in Teaching in Analytical Chemistry, Bratislava, Eslovaquia, Available from http://jchemed.chem.wisc.edu/JCEDLib/WebWare/collection/open/JCEWWOR 012/

Urbansky, E. & Schock, M. R. (2000). Understanding, Deriving, and Computing Buffer Capacity. *Journal of Chemical Education*, Vol.77, pp. 1640-1644

Van Slyke, D. D. (1922). On the Measurement of Buffer Values and on the Relationship of Buffer Values to the Dissociation Constant of the Buffer and the Concentration and Reaction of the Buffer Solution. *Journal of Biological Chemistry*, Vol. 52, pp. 525-570

Vicente-Pérez, S. (1985). *Química de las Disoluciones. Diagramas y Cálculos Gráficos*. Alhambra. Madrid, Spain
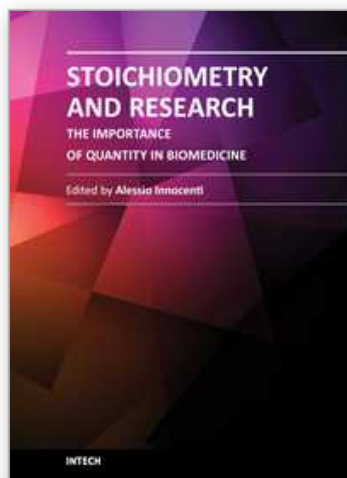
Stoichiometry and Research - The Importance of Quantity in Biomedicine
Edited by Dr Alessio Innocenti

The aim of this book is to provide an overview of the importance of stoichiometry in the biomedical field. It proposes a collection of selected research articles and reviews which provide up-to-date information related to stoichiometry at various levels. The first section deals with host-guest chemistry, focusing on selected calixarenes, cyclodextrins and crown ethers derivatives. In the second and third sections the book presents some issues concerning stoichiometry of metal complexes and lipids and polymers architecture. The fourth section aims to clarify the role of stoichiometry in the determination of protein interactions, while in the fifth section some selected experimental techniques applied to specific systems are introduced. The last section of the book is an attempt at showing some interesting connections between biomedicine and the environment, introducing the concept of biological stoichiometry. On this basis, the present volume would definitely be an ideal source of scientific information to researchers and scientists involved in biomedicine, biochemistry and other areas involving stoichiometry evaluation.

INTECH
open science | open minds